

See discussions, stats, and author profiles for this publication at: <https://www.researchgate.net/publication/11362402>

# DNA dynamics: A fluorescence resonance energy transfer study using a long-lifetime metal-ligand complex

ARTICLE *in* ARCHIVES OF PHARMACAL RESEARCH · MAY 2002

Impact Factor: 2.05 · DOI: 10.1007/BF02976554 · Source: PubMed

---

CITATIONS

12

---

READS

27

3 AUTHORS, INCLUDING:



[Joseph R Lakowicz](#)

University of Maryland Medical Center

876 PUBLICATIONS 42,113 CITATIONS

SEE PROFILE

## DNA Dynamics: a Fluorescence Resonance Energy Transfer Study Using a Long-Lifetime Metal-Ligand Complex

Jung Sook Kang<sup>1</sup>, Joseph R. Lakowicz<sup>2</sup>, and Grzegorz Piszczek<sup>3</sup>

<sup>1</sup>Department of Oral Biochemistry and Molecular Biology, College of Dentistry and Research Institute for Oral Biotechnology, Pusan National University, Pusan 602-739, Korea, <sup>2</sup>Center for Fluorescence Spectroscopy, Department of Biochemistry and Molecular Biology, University of Maryland School of Medicine, Baltimore, MD 21201, U.S.A., <sup>3</sup>Institute of Experimental Physics, University of Gdańsk, ul. Wita Stwosza 57, 80-952 Gdańsk, Poland

(Received December 15, 2001)

Fluorescent probes bound to DNA typically display nanosecond decay times and reveal only nanosecond motions. We extend the time range of measurable DNA dynamics using  $[\text{Ru}(\text{bpy})_2(\text{dppz})]^{2+}$  (bpy=2,2'-bipyridine, dppz=dipyrido[3,2-a:2',3'-c]phenazine) (RuBD) which displays a mean lifetime near 90 ns. To test the usefulness of RuBD as a probe for diffusive processes in calf thymus DNA, we compared the efficiencies of fluorescence resonance energy transfer (FRET) using three donors which display lifetimes near 5 ns for acridine orange (AO), 22 ns for ethidium bromide (EB) and 92 ns for RuBD, with Nile blue (NB) as the acceptor. The Förster distances for AO-NB, EB-NB and RuBD-NB donor-acceptor pairs were 42.3, 52.3, and 30.6 Å, respectively. All three donors showed dramatic decreases in fluorescence intensities and more rapid intensity decays with increasing NB concentrations. The intensity decays of AO and EB in the presence of varying concentrations of NB were satisfactorily described by the one-dimensional FRET model without diffusion (Blumen and Manz, 1979). In the case of the long-lifetime donor RuBD, the experimental phase and modulation somewhat deviated from the recovered values computed from this model. The recovered NB concentrations and FRET efficiencies from the model were slightly larger than the expected values, however, the recovered and expected values did not show a significant difference. Thus, it is suggested that the lifetime of RuBD is too short to measure diffusive processes in calf thymus DNA.

**Key words:** Fluorescence resonance energy transfer, Long-lifetime metal-ligand complex, Diffusion in DNA, Frequency-domain fluorometry

### INTRODUCTION

Fluorescence resonance energy transfer (FRET) is a process by which the excited-state energy of a fluorescent donor molecule is nonradiatively transferred to an unexcited acceptor molecule by means of long-range dipole-dipole coupling. The rate of energy transfer depends upon the extent of spectral overlap of the emission spectrum of the donor with the absorption spectrum of the acceptor, the quantum yield of the donor, the relative orientation of the donor and acceptor transition dipoles, and the distance between the donor and acceptor molecules. Because of

the distance dependence, FRET has been extensively used as a "spectroscopic ruler" to measure distances between donors and acceptors and macromolecular associations in proteins (Steinberg, 1971; Stryer, 1978). Most of such applications of FRET involve molecules that are labeled with a single donor-acceptor pair.

However, the occurrence of random distributions of acceptors complicates energy transfer. In double-helical DNA, each donor sees a different acceptor population since the acceptors are randomly distributed in one-dimension along the DNA helix. One dimensional energy transfer in DNA was previously reported from dimethyldiazaperopyrenium to ethidium bromide (EB) (Mergny *et al.*, 1991), for a number of donor-acceptor pairs bound to DNA (Maliwal *et al.*, 1995) and from minor groove-binding Hoechst 33258 to intercalating propidium iodide (Murata *et al.*, 2000). The extent of energy transfer can be also influenced by the presence

Correspondence to: Jung Sook Kang, Department of Oral Biochemistry and Molecular Biology, College of Dentistry, Pusan National University, 1-10 Ami-dong, Seo-gu, Pusan 602-739, Korea  
E-mail: jsokang@pusan.ac.kr

of donor-to-acceptor diffusion during the donor lifetime. Diffusion-enhanced FRET from millisecond-lifetime lanthanide complexes has been well known (Stryer *et al.*, 1982). For the lifetimes of 1–20 ns displayed by most DNA fluorophores, there is little translational displacement during the lifetime of the donor. However, a number of long-lifetime metal-ligand complexes (MLCs) which display decay times ranging from 100 ns to more than 10  $\mu$ s have recently become available (DeGraff and Demas, 1994; Lakowicz *et al.*, 2000; Terpetschnig *et al.*, 1997). The longer donor decay times allow the excited donor molecule to diffuse through all allowed directions and orientations in space.

Long-lifetime MLCs show a variety of characteristics that make them useful probes. Because of the large Stokes' shift, the MLCs do not self-quench (Lakowicz *et al.*, 2000; Terpetschnig *et al.*, 1997). In general, the MLCs show good water solubility and high chemical and photochemical stability (Lakowicz *et al.*, 2000; Terpetschnig *et al.*, 1997). In contrast with lanthanide complexes, the MLCs display polarized emission, making them useful for microsecond dynamics (Lakowicz *et al.*, 2000; Terpetschnig *et al.*, 1997). Finally, the long lifetimes of the MLCs allow the use of gated detection, which can be employed to suppress interfering autofluorescence from biological samples and can thus provide increased sensitivity (Haugen and Lytle, 1981). Barton and coworkers (Friedman *et al.*, 1990; Jenkin *et al.*, 1992; Murphy and Barton, 1993) reported that the dipyrro[3,2-a:2',3'-c]phenazine (dppz) complexes of ruthenium appears to be a prime candidate for a spectroscopic probe for nucleic acids because of their "molecular light switch" properties for DNA. As interaction of water with the nitrogen atoms on the dppz quenches the luminescence, the ruthenium complexes display no detectable luminescence in aqueous solution, but they luminesce brightly in the presence of double-helical DNA.

Based upon the Förster model that the donor intensity decays are stretched exponential,  $\exp[-(t/\tau)^{d/6}]$ , where  $d$  is the dimension of the system, Blumen and Manz (1979) derived an equation for the ensemble averaged time decay of an excited donor in the presence of randomly distributed acceptors in one dimension in a lattice structure. Accordingly, in the absence of diffusion, the donor intensity decays in one dimension can be predicted using the Blumen and Manz's equation. In this study, using frequency-domain fluorometry, we compared the expected efficiencies of FRET in calf thymus DNA with the recovered values computed from the Blumen and Manz's equation without diffusion. We employed three donors which show lifetimes near 5 ns for acridine orange (AO), 22 ns for EB, and 92 ns for  $[\text{Ru}(\text{bpy})_2(\text{dppz})]^{2+}$  (bpy=2,2'-bipyridine) (RuBD) with Nile blue (NB) as the acceptor. The results suggest that

the lifetime of RuBD is too short to measure diffusive processes in DNA.

## MATERIALS AND METHODS

### Materials

Calf thymus DNA was obtained from Sigma (St. Louis, MO, USA). AO and EB were purchased from Molecular Probes (Eugene, OR, USA). RuBD was synthesized by the method described previously (Lakowicz *et al.*, 1995; Malak *et al.*, 1997), and NB was from Aldrich (Milwaukee, WI, USA). All reagents were used without further purification, and water was deionized with a Milli-Q system. To convert calf thymus DNA into linear fragments comparable in length to one persistent length, about 5 mg/ml solution of calf thymus DNA was sonicated approximately 10 min while submerged in an ice bath. The sonicated DNA solution was centrifuged for 1 hr at 75,000  $\times g$  to remove titanium tip particles and undissolved DNA. All experiments were undertaken at room temperature in 2 mM Tris-HCl, pH 8, containing 0.1 mM ethylenediaminetetraacetic acid.

### Absorption and steady-state fluorescence measurement

About 2–5 mM of stock solutions of AO, RuBD, and NB were prepared in dimethylformamide, and about 10 mM stock solution of EB was made in dimethylsulfoxide. The DNA concentration was 1 mM base pair (bp) while the concentrations of AO, EB, and RuBD were 5, 10, and 20  $\mu$ M, respectively. The concentrations of DNA and the acceptor NB were quantified using molar extinction coefficients of 13,300  $\text{M}^{-1}\text{cm}^{-1}$  (expressed as bp) at 260 nm and 42,900  $\text{M}^{-1}\text{cm}^{-1}$  at 656 nm, respectively. Concentrations of the donors were determined using the extinction coefficients in Table I. UV-visible absorption spectra were measured with a Hewlett-Packard 8453 diode array spectrophotometer. Steady-state fluorescence measurements were carried out using a Aminco-Bowman series 2 luminescence spectrometer (Spectronic Instruments, Inc., Rochester, NY, USA). The excitation wavelengths of AO, EB and RuBD were 480, 480 and 442 nm, respectively.

### Frequency-domain intensity decay measurements

Measurements were performed with the instruments described previously (Lakowicz and Maliwal, 1985) and modified with a data acquisition card from ISS, Inc. (Urbana, IL, USA) (Feddersen *et al.*, 1989). For AO, the excitation source was a cavity-dumped output of a synchronously pumped pyridine-2 dye laser, generating a

laser pulse train with a repetition rate of 3.81 MHz and the pulse width of about 7 ps. The dye laser output was frequency doubled to 370 nm, and the AO emission was isolated using a  $520 \pm 10$  nm interference filter. The detection was a Hamamatsu R2809 microchannel plate photomultiplier tube. For EB, the light source was a continuous wave argon ion laser at 514 nm and modulated with a Pockels cell, and the emission was isolated using a  $600 \pm 20$  nm interference filter. In the case of RuBD, the excitation source was a blue light-emitting diode (LED) LNG992CFBW (Panasonic, Japan) with luminous intensity of 1,500 mcd. An LED driver LDX-3412 (ILX Lightwave, Boseman, MO, USA) provided 30 mA of current at frequencies from 0.5 to 15 MHz. A  $450 \pm 20$  nm interference filter and a 620 nm cut-off filter were used for isolating excitation and emission, respectively. The lifetime standard for AO was 4-dimethylamino-4'-cyanostilbene in methanol ( $\tau = 0.46$  ns), and that for EB and RuBD was rhodamine B in water ( $\tau = 1.68$  ns).

The intensity decays were initially analyzed from the frequency-domain data in terms of a multiexponential model:

$$I(t) = \sum_{i=1}^n \alpha_i e^{-t/\tau_i} \quad (1)$$

where the preexponential factors  $\alpha_i$  are amplitudes of each component,  $\sum \alpha_i = 1.0$ ,  $\tau_i$  are the decay times, and  $n$  are the numbers of exponential components. These values were determined by nonlinear least squares analysis as described previously (Gratton *et al.*, 1984; Lakowicz *et al.*, 1984). Mean lifetimes were calculated according to:

$$\langle \tau \rangle = \frac{\sum \alpha_i \tau_i^2}{\sum \alpha_i \tau_i} = \sum f_i \tau_i \quad (2)$$

where  $f_i$  is the fractional steady-state contribution of each component to the total emission, and  $\sum f_i$  is normalized to unity.  $f_i$  is given by

$$f_i = \frac{\alpha_i \tau_i}{\sum_j \alpha_j \tau_j} \quad (3)$$

The best fits were obtained by minimizing  $\chi_R^2$  values:

$$\chi_R^2 = \frac{1}{v} \sum_w \left[ \left( \frac{\varphi_w - \varphi_{cw}}{\delta \varphi} \right)^2 + \left( \frac{m_w - m_{cw}}{\delta m} \right)^2 \right] \quad (4)$$

where  $v$  is the number of degrees of freedom, and  $\varphi_w$  and  $m_w$  are the experimental phase and modulation, respectively. The subscript  $c$  is used to indicate calculated values for assumed values of  $\alpha_i$  and  $\tau_i$ , and  $\delta \varphi$  and  $\delta m$  are the experimental uncertainties.

## THEORY

Additional insights into the presence of FRET in DNA can be obtained using a model for energy transfer in one dimension. For an isolated donor-acceptor pair the energy transfer rate  $k_T(r)$  averaged over all the orientations is given by

$$k_T(r) = \frac{1}{\tau_D} \left( \frac{R_0}{r} \right)^6 \quad (5)$$

where  $\tau_D$  is the decay time of the donor in the absence of acceptor,  $R_0$  is the Förster distance, and  $r$  is the donor-acceptor distance. The Förster distance  $R_0$  is the distance at which FRET is 50% efficient and given by

$$R_0 = (J(\lambda) \kappa^2 Q_D n^{-4})^{1/6} \times 9.78 \times 10^3 \text{ Å} \quad (6)$$

where  $J(\lambda)$  is the spectral overlap integral of donor emission and acceptor absorption,  $\kappa^2$  is the orientation factor for dipole-dipole interaction and taken as 1.25 (Maliwal *et al.*, 1995; Murata *et al.*, 2000),  $Q_D$  is quantum yield of the donor in the absence of acceptor, and  $n$  is the refractive index of the medium and assumed to be 1.5 (Maliwal *et al.*, 1995; Murata *et al.*, 2000). The overlap integral  $J(\lambda)$  expresses the degree of spectral overlap between the donor emission and the acceptor absorption

$$J(\lambda) = \int_0^\infty F_D(\lambda) \varepsilon_A(\lambda) \lambda^4 d\lambda \quad (7)$$

where  $F_D(\lambda)$  is the corrected fluorescence intensity of the donor in the wavelength range  $\lambda$  to  $\lambda + \Delta\lambda$ , with the total intensity (area under the curve) normalized to unity, and  $\varepsilon_A(\lambda)$  is the extinction coefficient of the acceptor at  $\lambda$ , which is typically in the unit of  $M^{-1} \text{ cm}^{-1}$ .

A model for FRET in one dimension was reported by Blumen and Manz (1979). When a donor is surrounded by randomly distributed acceptors on a lattice structure, they showed that the intensity decays of the donor in one dimension can be described as follows:

$$\log I(T) = -T + \frac{\rho}{C_0} T^{1/6} \sum_{k=1}^\infty \frac{1}{k} \left( \frac{C_A}{\rho} \right)^k \times \left[ \lambda^{1/6} + (1 - e^{-\lambda})^k + \sum_{L=1}^k (-1)^L \binom{k}{L} L^{1/6} \gamma\left(\frac{5}{6}, L\lambda\right) \right] \quad (8)$$

where  $T = t/\tau$ ,  $\rho$  is the density of lattice points in the particular lattice considered,  $C_0 = (2R_0)^{-1}$  is the critical concentration for dipole-dipole energy transfer from donor to acceptor,  $C_A$  is the acceptor concentration in unit length,  $\lambda = T(R_0/r_{min})^6$ ,  $r_{min}$  is the minimal donor-acceptor distance and assumed to be 6.8 Å because of the length of a bp 3.4 Å (Maliwal *et al.*, 1995), and  $\gamma(a, x)$  is the incomplete gamma function. The efficiency of FRET ( $E$ ) is the fraction of photons absorbed by the donor that are transferred to

$$E = 1 - \frac{\sum_i \alpha_i \tau_i \int_0^{\infty} I(T) dT}{\sum_i \alpha_i \tau_i} \quad (9)$$

## RESULTS AND DISCUSSION

We chose dyes non-covalently bound to DNA, and the chemical structures of three donors and the acceptor NB are shown in Fig. 1. The absorption and emission spectra of AO-NB, EB-NB and RuBD-NB donor-acceptor pairs are shown in Fig. 2. As can be seen, all three donor-acceptor pairs showed a significant overlap of the emission spectra of the donors with the absorption spectra of the

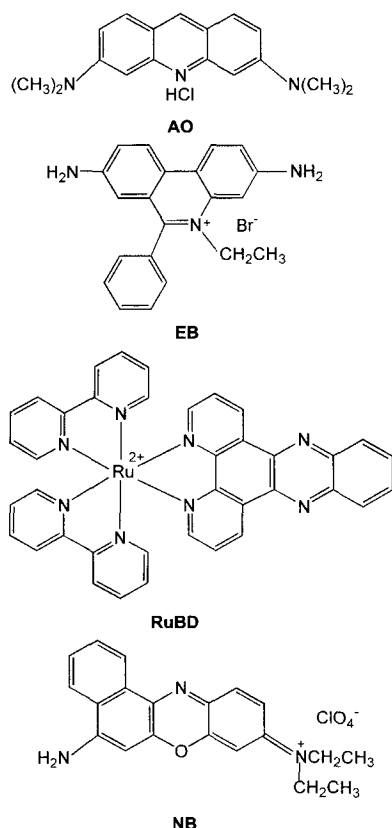


**Fig. 1.** Chemical structures of the three donors and the acceptor NB

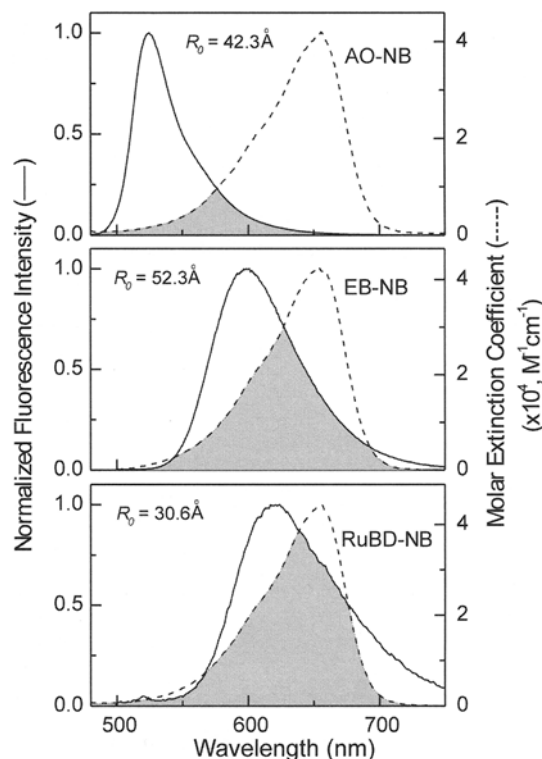


**Fig. 2.** Emission spectra (—) of AO (top), EB (middle), and RuBD (bottom) and absorption spectra (---) of the acceptor NB intercalated into calf thymus DNA. The spectral overlaps shown in gray were used to calculate the Förster distance  $R_0$ .

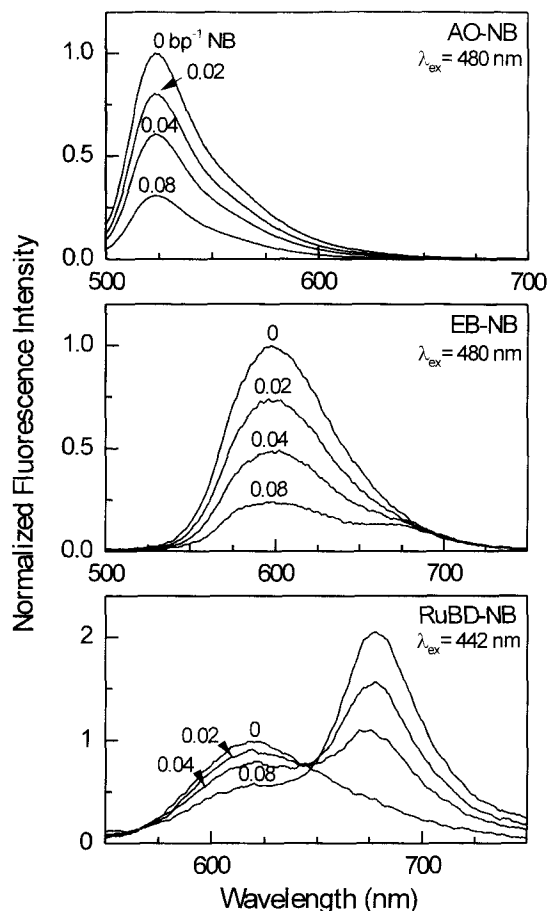
acceptor. The spectral overlap integrals ( $J(\lambda)$ ) were used to calculate the Förster distances  $R_0$  according to Eq. (6), and the results are summarized in Table I. The Förster distances for AO-NB, EB-NB and RuBD-NB donor-acceptor pairs were 42.3, 52.3 and 30.6 Å, respectively. The steady-state fluorescence intensities of AO, EB and RuBD decreased dramatically with an increase in NB concentration (Fig. 3). One also observes increasing emission from the NB acceptor centered about 676 nm in the case of low quantum yield donor RuBD (Fig. 3, bottom panel). Recently we showed that the enhancement of the acceptor emission from FRET is larger for RuBD, a low quantum yield donor ( $Q=0.008$ , Table I) than for high quantum yield donors AO ( $Q=0.392$ , Table I) and EB

Table I. Molar extinction coefficients ( $\epsilon$ ), donor quantum yields ( $Q_D$ ), spectral overlap integrals ( $J(\lambda)$ ) and Förster distances ( $R_0$ ) in calf thymus DNA

Donor	$\varepsilon/\lambda_{\text{max}}$ ( $\text{M}^{-1}\text{cm}^{-1}/\text{nm}$ )	$Q_D^a$	$J(\lambda)^b$ ( $\times 10^{-13}$ , $\text{M}^{-1}\text{cm}^3$ )	$R_D^b$ ( $\text{\AA}$ )
AO	5,300/500	0.392	0.676	42.3
EB	5,200/518	0.219	4.332	52.3
RuBD	13,000/440	0.008	4.708	30.6

<sup>a</sup>From Lakowicz *et al.* (2001).

<sup>b</sup>  $J(\lambda)$  and  $R_0$  were calculated by Eqs. (7) and (6), respectively.



**Fig. 3.** Emission spectra of AO-NB (top), EB-NB (middle), and RuBD-NB (bottom) donor-acceptor pairs intercalated into calf thymus DNA.

( $Q=0.219$ , Table I) (Lakowicz *et al.*, 2001). If the acceptor does not absorb at the excitation wavelength, the enhancement is inversely proportional to the quantum

yield of the donor (Kang and Lakowicz, 2001).

### Time-resolved donor intensity decays

The donor intensity decays were measured using the frequency-domain method, and the frequency responses of AO, EB and RuBD intercalated into DNA in the absence of the NB acceptor are shown in Fig. 4 (open circles). The frequency-domain intensity decays of donors were first analyzed in terms of the multiexponential model according to Eqs. (1)-(4) (Table II). In the absence of the acceptor NB, the intensity decays of AO-calf thymus DNA complex were monoexponential with a lifetime of about 5.0 ns. EB displays a double exponential decay with a mean decay time of 21.9 ns. The RuBD intensity decay was more heterogeneous and required three lifetime components with a mean decay time of 91.7 ns ( $\chi_R^2=1.5$ ). For all three donors, the intensity decays became faster and somewhat more heterogeneous upon adding the acceptor NB. As the acceptor concentration increases, the frequency responses of all donors shift to higher modulation frequencies (Fig. 4, closed symbols), which indicates a decrease in the mean decay times. In the presence of 100  $\mu$ M NB acceptor, the mean decay times of AO, EB, and RuBD decreased to 3.3, 13.5, and 61.1 ns, respectively (Table II). The heterogeneity upon FRET occurs because a distribution of donor-to-acceptor distances results in a wider range of donor decay times. In the case of AO, the donor intensity decay displayed a triple exponential decay in the presence of the NB acceptor (Table II). For EB, three decay times were needed to fit the data for donor-acceptor pairs (Table II). In the presence of the NB acceptor, RuBD showed a triple exponential decay, however,  $\chi_R^2$  values for the fit increased to 3.1, 4.8 and 5.3, respectively, in the presence of 60, 80

**Table II.** Multiexponential intensity decay analyses of the three donors and the NB acceptor intercalated into calf thymus DNA

Donor	NB Conc. (bp <sup>-1</sup> )	$\tau_1$ (ns)	$\alpha_1$	$f_1^a$	$\tau_2$ (ns)	$\alpha_2$	$f_2^a$	$\tau_3$ (ns)	$\alpha_3$	$f_3^a$	$\langle\tau\rangle^a$ (ns)	$\chi_R^2$ <sup>b</sup>
AO	0	4.98	1	1.00	—	—	—	—	—	—	4.98	2.27
	0.06	4.47	0.51	0.84	1.48	0.25	0.14	0.23	0.24	0.02	3.97	1.69
	0.08	4.40	0.35	0.76	1.43	0.28	0.20	0.21	0.37	0.04	3.65	0.94
	0.10	4.04	0.31	0.77	1.11	0.27	0.19	0.16	0.42	0.04	3.33	2.27
EB	0	23.41	0.76	0.84	14.00	0.24	0.16	—	—	—	21.90	1.65
	0.06	21.43	0.28	0.61	9.35	0.35	0.33	1.58	0.37	0.06	16.25	0.79
	0.08	19.83	0.23	0.64	6.55	0.34	0.30	1.02	0.43	0.06	14.64	1.58
	0.10	18.51	0.21	0.63	5.94	0.29	0.28	1.11	0.50	0.09	13.47	0.93
RuBD	0	111.41	0.27	0.64	49.96	0.30	0.31	5.52	0.43	0.05	91.69	1.53
	0.06	92.26	0.23	0.69	34.39	0.19	0.22	4.37	0.58	0.09	71.91	3.10
	0.08	89.29	0.18	0.59	42.60	0.19	0.29	5.46	0.63	0.12	65.71	4.77
	0.10	84.90	0.17	0.61	34.18	0.18	0.25	5.26	0.65	0.14	61.05	5.25

<sup>a</sup>Fractional intensities  $f_i$  and mean lifetimes  $\langle\tau\rangle$  were calculated according to Eqs. (3) and (2), respectively.

<sup>b</sup>The  $\chi_R^2$  values were calculated by Eq. (4), and the standard errors of phase angle and modulation were set at 0.2° and 0.005, respectively.

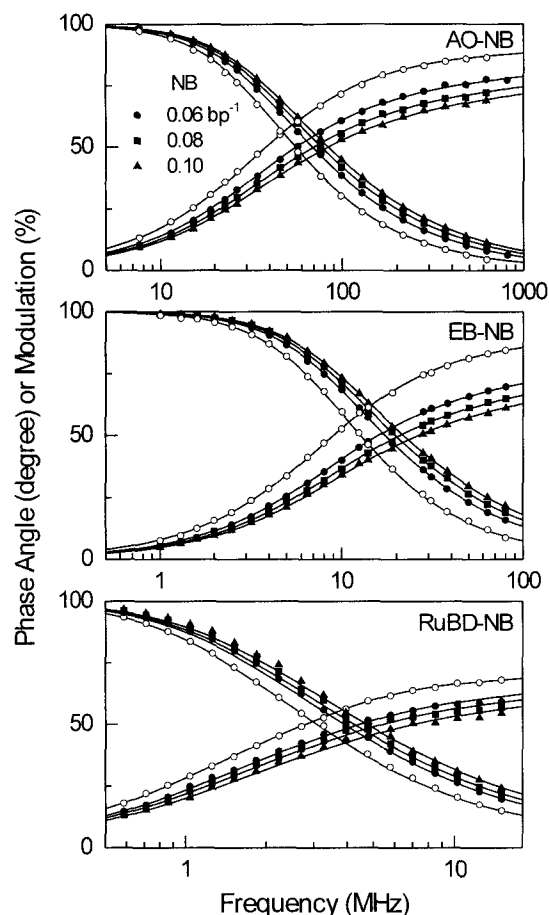


**Fig. 4.** Frequency-domain intensity decays of AO (top), EB (middle), and RuBD (bottom) intercalated into calf thymus DNA in the absence (open circles) and presence (closed symbols) of varying concentrations of the acceptor NB. The intensity decay data were globally analyzed according to the one-dimensional FRET model without diffusion using Eq. (8) with acceptor concentrations as variable parameters. The symbols represent the measured phase and modulation values, and the solid lines show the best global fits according to this model.

and 100 bp<sup>-1</sup> NB (Table II). The donor intensity decays could be still more complex because it is almost impractical to resolve the intensity decay data into more than three exponential components (Small and Isenberg, 1977)

### FRET in one dimension

The intensity decays of donors were then analyzed by the one-dimensional FRET model without donor-to-acceptor diffusion according to Eq. (8) (Blumen and Manz, 1979). The intensity decays of both AO (Fig. 4, top panel) and EB (Fig. 4, middle panel) in the presence of varying concentrations of NB were satisfactorily described by this model. At the concentrations of 0.06, 0.08 and 0.10 bp<sup>-1</sup> NB, the recovered NB concentrations

**Table III.** Comparison between the expected and recovered acceptor NB concentrations

Donor	[NB] (bp <sup>-1</sup> )		$\chi_R^2$	
	Expected <sup>a</sup>	Recovered <sup>b</sup>	Expected	Recovered
AO	0.06	0.053	5.6	1.0
	0.08	0.077		
	0.10	0.094		
EB	0.06	0.059	1.7	0.4
	0.08	0.079		
	0.10	0.094		
RuBD	0.06	0.062	6.0	5.3
	0.08	0.082		
	0.10	0.106		

<sup>a</sup>Determined by using  $\epsilon=42,900 \text{ M}^{-1}\text{cm}^{-1}$  at 656 nm.

<sup>b</sup>Computed using Eq. (8) by globally fitting the frequency-domain intensity decay data to [NB]. For AO, the input parameters for the computation were  $\tau=5.0 \text{ ns}$ ,  $R_0=42.3 \text{ \AA}$ ,  $r_{\text{min}}=6.8 \text{ \AA}$ , and the expected [NB]. In the case of EB, we used the same input parameters except  $\tau=21.9 \text{ ns}$  and  $R_0=52.3 \text{ \AA}$ . The same parameters were employed for RuBD except  $\tau=91.7 \text{ ns}$  and  $R_0=30.6 \text{ \AA}$ .

<sup>c</sup>The expected and recovered  $\chi_R^2$  values were obtained before and after globally fitting the frequency-domain intensity decay data to [NB] using Eq. (8), respectively. The above input parameters were employed for the computation. The  $\chi_R^2$  values were calculated by Eq. (4), and the standard errors of phase angle and modulation were set at 0.3° and 0.008, respectively.

**Table IV.** Comparison between the expected and recovered FRET efficiencies ( $E$ )<sup>a</sup>

Donor	[NB] (bp <sup>-1</sup> )	$E^b$	
		Expected	Recovered
AO	0.06	0.66	0.62
	0.08	0.76	0.75
	0.10	0.83	0.81
EB	0.06	0.75	0.74
	0.08	0.84	0.84
	0.10	0.90	0.88
RuBD	0.06	0.58	0.59
	0.08	0.68	0.69
	0.10	0.76	0.78

<sup>a</sup>All conditions are the same as those in Table III.

<sup>b</sup>The expected and recovered  $E$  values were obtained before and after globally fitting the frequency-domain intensity decay data to [NB] using Eq. (8), respectively. The  $E$  values were calculated by Eq. (9).

from this model were somewhat lower than the expected values determined by using molar extinction coefficient of NB ( $\epsilon_{656 \text{ nm}} = 42,900 \text{ M}^{-1}\text{cm}^{-1}$ ) (Table III). The recovered FRET efficiencies from the one-dimensional FRET model were also slightly lower than the expected values (Table IV). For the long-lifetime donor RuBD, the experimental phase and modulation (Fig. 4, symbols in bottom panel) somewhat deviated from the recovered



values computed from the model using Eq. (8) (Fig. 4, solid lines in bottom panel). In addition, we observed slightly larger values of recovered NB concentrations and FRET efficiencies than the expected values (Tables III and IV). However, the recovered and expected values of NB concentrations and FRET efficiencies did not show a significant difference. It is well known that donor-acceptor diffusion increases the efficiency of energy transfer between covalently linked donor-acceptor pairs (Lakowicz *et al.*, 1994) and in homogenous solution (Steinberg and Katchalski, 1968). Thus, it is suggested that, although RuBD showed a slightly different energy transfer property from AO and EB, it seems that the lifetime of RuBD ( $\tau = 91.7$  ns, Table II) is too short to measure diffusive processes in DNA. The use of long-lifetime MLCs to measure DNA dynamics is just beginning, and additional MLCs with longer lifetime and higher quantum yield are yet to be developed.

## ACKNOWLEDGEMENTS

JSK thanks Professor Ignacy Gryczynski, Center for Fluorescence Spectroscopy, for valuable advice. This work was supported by the NIH, National Center for Research Resources, RR 08119.

## REFERENCES

- Blumen, A. and Manz, J., On the concentration and time dependence of the energy transfer to randomly distributed acceptors. *J. Chem. Phys.*, 71, 4694-4702 (1979).
- DeGraff, B. A. and Demas, J. N., Direct measurement of rotational correlation times of luminescent ruthenium(II) molecular probes by differential polarized phase fluorometry. *J. Phys. Chem.*, 98, 12478-12480 (1994).
- Feddersen, B. A., Piston, D. W. and Gratton, E., Digital parallel acquisition in frequency domain fluorimetry. *Rev. Sci. Instrum.*, 60, 2929-2936 (1989).
- Friedman, A. E., Chambron, J.-C., Sauvage, J.-P., Turro, N. J. and Barton, J. K., Molecular "light switch" for DNA: Ru(bpy)<sub>2</sub>(dppz)<sup>2+</sup>. *J. Am. Chem. Soc.*, 112, 4960-4962 (1990).
- Gratton, E., Lakowicz, J. R., Maliwal, B. P., Cherek, H. and Laczko, G., Resolution of mixtures of fluorophores using variable-frequency phase and modulation data. *Biophys. J.*, 46, 478-486 (1984).
- Haugen, G. R. and Lytle, F. E., Quantitation of fluorophores in solution by pulsed laser excitation and time-filtered detection. *Anal. Chem.*, 53, 1554-1559 (1981).
- Jenkin, Y., Friedman, A. E., Turro, N. J. and Barton, J. K., Characterization of dipyrrophenazine complexes of ruthenium(II): The light switch effect as a function of nucleic acid sequence and conformation. *Biochemistry*, 31, 10809-10816 (1992).
- Kang, J. S. and Lakowicz, J. R., Fluorescence resonance energy transfer in calf thymus DNA from a long-lifetime metal-ligand complex to nile blue. *J. Biochem. Mol. Biol.*, 34, 551-558 (2001).
- Lakowicz, J. R., Gratton, E., Laczko, G., Cherek, H. and Limkeman, M., Analysis of fluorescence decay kinetics from variable-frequency phase shift and modulation data. *Biophys. J.*, 46, 463-477 (1984).
- Lakowicz, J. R., Gryczynski, I., Kuśba, J., Wiczak, W., Szmajda, H. and Johnson, M. L., Site-to-site diffusion in proteins as observed by energy transfer and frequency domain fluorometry. *Photochem. Photobiol.*, 59, 16-29 (1994).
- Lakowicz, J. R., Gryczynski, I., Piszczek, G., Tolosa, L., Nair, R., Johnson, M. L. and Nowaczyk, K., Microsecond dynamics of biological macromolecules. *Methods Enzymol.*, 323, 473-509 (2000).
- Lakowicz, J. R., Malak, H., Gryczynski, I., Castellano, F. N. and Meyer, G. J., DNA dynamics observed with long lifetime metal-ligand complexes. *Biospectroscopy*, 1, 163-168 (1995).
- Lakowicz, J. R. and Maliwal, B. P., Construction and performance of a variable-frequency phase-modulation fluorometer. *Biophys. Chem.*, 21, 61-78 (1985).
- Lakowicz, J. R., Piszczek, G. and Kang, J. S., On the possibility of long-wavelength long-lifetime high quantum-yield luminophores. *Anal. Biochem.*, 288, 62-75 (2001).
- Malak, H., Gryczynski, I., Lakowicz, J. R., Meyers, G. J. and Castellano, F. N., Long-lifetime metal-ligand complexes as luminescent probes for DNA. *J. Fluorescence*, 7, 107-112 (1997).
- Maliwal, B. P., Kuśba, J. and Lakowicz, J. R., Fluorescence energy transfer in one dimension: frequency-domain fluorescence study of DNA-fluorophore complexes. *Biopolymers*, 35, 245-255 (1995).
- Mergny, J. L., Slama-Schwok, A., Montenay-Garestier, T., Rougee, M. and Helene, C., Fluorescence energy transfer between dimethyldiazaperopyrenium dication and ethidium intercalated in poly d(A-T). *Photochem. Photobiol.*, 53, 555-558 (1991).
- Murata, S. I., Kuśba, J., Piszczek, G., Gryczynski, I. and Lakowicz, J. R., Donor fluorescence decay analysis for energy transfer in double-helical DNA with various acceptor concentrations. *Biopolymers*, 57, 306-315 (2000).
- Murphy, C. J. and Barton, J. K., Ruthenium complexes as luminescent reporters of DNA. *Methods Enzymol.*, 226, 576-594 (1993).
- Small, E. W. and Isenberg, I., Hydrodynamics properties of a rigid molecule: Rotational and linear diffusion and fluorescence anisotropy. *Biopolymers*, 16, 1907-1928 (1977).
- Steinberg, I. Z., Long-range nonradiative transfer of electronic excitation energy in proteins and polypeptides. *Ann. Rev. Biochem.*, 40, 83-114 (1971).
- Steinberg, I. Z. and Katchalski, E., Theoretical analysis of the role of diffusion in chemical reactions, fluorescence quenching,



- and nonradiative energy transfer. *J. Chem. Phys.*, 48, 2404-2410 (1968).
- Stryer, L., Fluorescence energy transfer as a spectroscopic ruler. *Ann. Rev. Biochem.*, 47, 819-846 (1978).
- Stryer, L., Thomas, D. D. and Meares, C. F., Diffusion-enhanced fluorescence energy transfer. *Ann. Rev. Biophys. Bioeng.*, 11, 203-222 (1982).
- Terpetschnig, E., Szmecinski, H. and Lakowicz, J. R., Long-lifetime metal-ligand complexes as probes in biophysics and clinical chemistry. *Methods Enzymol.*, 278, 295-321 (1997).